The American Journal of Pathology, Vol. 173, No. 4, October 2008

DOI: 10.2353/ajpath.2008.071034

Cardiovascular, Pulmonary and Renal Pathology

CX3CL1 Up-Regulation Is Associated with Recruitment of CX3CR1$^+$ Mononuclear Phagocytes and T Lymphocytes in the Lungs during Cigarette Smoke-Induced Emphysema

Jennifer G. McComb,* Mrunalini Ranganathan,* Xiang Hong Liu,* Joseph M. Pilewski,* Prabir Ray,* Simon C. Watkins,† Augustine M.K. Choi,* and Janet S. Lee*

From the Department of Medicine, Division of Pulmonary, Allergy, and Critical Care Medicine, the Department of Cell Biology and Physiology, and the Center for Biological Imaging,† University of Pittsburgh, Pittsburgh, Pennsylvania*

CX3CR1 is expressed on monocytes, dendritic cells, macrophages, subsets of T lymphocytes, and natural killer cells and functions in diverse capacities such as leukocyte adhesion, migration, and cell survival on ligand binding. Expression of the CX3CL1 gene, whose expression product is the sole ligand for CX3CR1, is up-regulated in human lungs with chronic cigarette smoke-induced obstructive lung disease. At present, it is unknown whether CX3CL1 up-regulation is associated with the recruitment and accumulation of immune cells that express CX3CR1. We show that mice chronically exposed to cigarette smoke up-regulate CX3CL1 gene expression, which is associated with an influx of CX3CR1$^+$ cells in the lungs. The increase in CX3CR1$^+$ cells is primarily comprised of macrophages and T lymphocytes and is associated with the development of emphysema. In alveolar macrophages, cigarette smoke exposure increased the expression of both CX3CR1 and CX3CL1 genes. The inducibility of CX3CR1 expression was not solely dependent on a chronic stimulus because lipopolysaccharide up-regulated CX3CR1 in RAW264.7 cells *in vitro* and in mononuclear phagocytes *in vivo*. Our findings suggest a mechanism by which macrophages amplify and promote CX3CR1$^+$ cell accumulation within the lungs during both acute and chronic inflammatory stress. We suggest that one function of the CX3CR1-CX3CL1 pathway is to recruit and sustain divergent immune cell populations implicated in the pathogenesis of cigarette smoke-induced emphysema. *(Am J Pathol 2008, 173:949–961; DOI: 10.2353/ajpath.2008.071034)*

Chronic obstructive pulmonary disease (COPD) is one of the leading causes of morbidity and mortality in the United States and is the only leading cause of death that continues to increase in prevalence.[1,2] The disease is characterized by a local inflammatory process that is associated with formation of mucous exudates within the lumens of small airways[3] and lung parenchymal destruction leading to airspace enlargement.[4] Cigarette smoking is the major risk factor for the development of COPD, and COPD severity in smokers is associated with the accumulation of neutrophils,[5] macrophages,[6] natural killer (NK) cells,[7] and T lymphocytes[8–10] in the peripheral airways and lung parenchyma. In particular, T lymphocyte and macrophage accumulation has been associated with worsening obstructive lung disease. These cells can release inflammatory mediators and/or proteinases which are thought to be responsible for the progressive parenchymal destruction in COPD.[11,12] The factors that regulate the recruitment and accumulation of these immune cells into the lungs in response to chronic cigarette smoke exposure remain poorly understood.

Recent studies suggest that chemokines and chemokine receptors play important roles in the recruitment of specific immune cell populations to the lungs. In smokers with COPD, increased CCL20 expression in the small airways has been shown to be associated with the accumulation of dendritic cells when compared to never smokers and to smokers without COPD.[13] Bracke and colleagues[14] recently showed that CCR6, the receptor for CCL20, contributes to cigarette smoke-induced inflammation and emphysema in mice. Other studies demonstrated that there is an increase in the number of CXCR3$^+$ T lymphocytes in the peripheral airways of smokers with

Supported by the American Thoracic Society (Innovative Research in COPD award) and HL086884.

Accepted for publication June 26, 2008.

Address reprint requests to Janet S. Lee, M.D., Division of Pulmonary, Allergy, and Critical Care Medicine, NW 628 Montefiore University Hospital, 3459 Fifth Ave., Pittsburgh, PA 15213. E-mail: leejs3@upmc.edu.

COPD[15] and an increase in the secretion of CXCR3 ligands, CXCL9 and CXCL10, in the lungs.[16] Although CCR6 and CXCR3 may be involved in immune cell accumulation in the peripheral airways of individuals with COPD, we do not have a complete understanding of the factors that regulate the recruitment of specific cell populations in COPD lungs.

Recent comprehensive gene expression profiling has shown an increase in CX3CL1 (also known as fractalkine or mouse neurotactin) expression in the lung tissues of smokers with COPD when compared to smokers without COPD.[17] Among the 327 differentially expressed genes, CX3CL1 was the only chemokine found to be up-regulated.[17] CX3CL1 is a unique molecule that exists as both a membrane-bound protein and a soluble chemokine.[18] The membrane-anchored protein is expressed on inflamed endothelium,[19,20] epithelial cells,[21] dendritic cells,[22] and neurons[23] and can mediate leukocyte adhesion.[19] Soluble CX3CL1 is released from the cell membrane through proteolytic cleavage and can function as an effective chemoattractant.[24,25] CX3CR1, the sole receptor for CX3CL1, is a seven-transmembrane, G-protein-coupled receptor that is expressed by cytotoxic effector $CD8^+$ and $CD4^+$ T lymphocytes in addition to $\gamma\delta$ T lymphocytes, NK cells, dendritic cells, and monocytes.[26–28]

Although the role of the CX3CL1-CX3CR1 pathway in the inflammatory process of COPD has never been evaluated, this ligand-receptor pair has been investigated in other inflammatory disease states. Local and systemic inflammation play critical roles in the development of atherosclerotic plaques, and macrophages are prominent in these lesions. The deletion of *cx3cl1* on an $apoE^{-/-}$ background decreased the size of brachiocephalic artery atherosclerotic lesions by 85% when compared to the wild-type mice,[29] and the deletion of *cx3cr1* on an $apoE^{-/-}$ background afforded significant protection from macrophage recruitment and atherosclerotic plaque formation.[30] These results suggest that $CX3CR1^+$ macrophages are playing a vital role in the development of early atherosclerotic lesions.

Bjerkeli and colleagues[31] showed that patients with Wegener's granulomatosis have increased levels of plasma CX3CL1 as well as enhanced gene expression of CX3CR1 in peripheral blood mononuclear cells. In addition, $CX3CR1^+$ peripheral blood mononuclear cells and T lymphocytes from patients with Wegener's granulomatosis secreted more inflammatory chemokines and showed increased chemotactic and adhesive responses to CX3CL1.[31] Yano and colleagues[32] found high levels of soluble CX3CL1 in the synovial fluid of patients with rheumatoid arthritis, and $CD16^+$ monocytes, expressing high levels of CX3CR1, were localized to the synovial lining and sublining layers. These authors suggest that CX3CL1 may promote the migration of $CD16^+/CX3CR1^+$ monocytes into the synovial tissues of patients with rheumatoid arthritis and may contribute to the tissue injury and joint destruction.[32]

Given these findings, we hypothesized that $CX3CR1^+$ cells comprise the inflammatory response in the lungs to chronic cigarette smoke exposure. We used a murine model of environmental tobacco smoke exposure and show increases in CX3CR1 expression in the lungs of animals with emphysema. We immunophenotyped $CX3CR1^+$ cells to the T-lymphocyte and macrophage populations and demonstrate the inducibility of CX3CR1 expression by resident mononuclear phagocytes of the lungs during both acute and chronic inflammatory stimuli.

Materials and Methods

Chronic Cigarette Exposure Model

A detailed method of our chronic cigarette exposure method has been previously described.[33] Briefly, total body cigarette smoke exposure was performed in a stainless steel chamber using a smoking machine (model TE-10; Teague Enterprises, Woodland, CA) similar to that reported by others.[34–36] The cigarette smoking machine puffed each 1R3F research cigarette for 2 seconds, for a total of nine puffs before ejection, at a flow rate of 1.05 L/minute, providing a standard puff of 35 cm^3. The smoke machine was adjusted to deliver five cigarettes at one time. The cigarette smoke from 80 cigarettes was delivered to the mice each day, 5 days/week for up to 24 weeks. The daily exposure time was ~3 to 4 hours per day. Age-, gender-, and strain-matched mice served as controls and were exposed to only filtered air in an identical body exposure chamber for a similar period of time. The smoking chamber atmosphere was periodically measured for total particulate matter concentrations of ~100 to 120 mg/m^3. After 2 weeks of cigarette exposure, carboxyhemoglobin levels in mice, immediately after exposure, were less than 8%. The body weights of the mice were measured weekly. The animals were sacrificed at 12- and 24-week time points.

Animals

Animal experiments were conducted in accordance with the Institutional Animal Care and Use Committee at the University of Pittsburgh. At 8 weeks of age, male AKR/J mice (The Jackson Laboratory, Bar Harbor, ME) were divided into air-exposed control animals and cigarette-exposed animals. The animals underwent the chronic exposure model as described above. Age-, gender-, and strain-matched male B6.129P-*cx3cr1*^{tm1Litt}/J mice (The Jackson Laboratory) were also used for immunofluorescence studies of the lungs. B6.129P-*cx3cr1*^{tm1Litt}/J mice were homozygous for a targeted mutation at the *cx3cr1* loci and expressed the enhanced green fluorescent protein (EGFP) instead of the endogenous gene.[37]

Mouse Necropsies

Lung Tissue Processing

The method of mouse necropsy has been previously described.[38] Briefly, animals were euthanized with an intraperitoneal, overdose injection of pentobarbital of 100 mg/kg. The thorax was opened, and the trachea was identified and cannulated with a 20-gauge angiocatheter.

The left hilum was identified and ligated with a 2-0 silk suture. The left lung was removed and immediately frozen in liquid nitrogen for subsequent RNA studies. The right lung was inflated by gravity with 4% paraformaldehyde in phosphate-buffered saline (PBS) and was held at a pressure of 30 cm H_2O for 15 minutes. The right lung was gently dissected from the thorax and placed in 4% paraformaldehyde in PBS for 6 to 8 hours. The samples were cut para-sagittally and embedded in paraffin. Paraffin-embedded sections were cut to ~5 μm thickness.

To obtain whole lungs for frozen tissue sections, the trachea was cannulated with an 18-gauge angiocatheter and up to 2.5 ml of Tissue-Tek O.C.T. compound (Sakura Finetek, Torrance, CA) was slowly instilled into both lungs. The trachea was ligated with a 2-0 silk suture, and the lungs were carefully dissected from the thorax. The instilled lungs were mounted in O.C.T. compound, and cryomolds were slowly frozen in liquid nitrogen. Frozen sections were cryosectioned to ~5 μm thickness.

Bronchoalveolar Lavage (BAL) of Whole Lung

The animals were euthanized, and the thorax was opened as described above. The trachea was identified and cannulated with an 18-gauge angiocatheter, and sequential lavages of 1.2 ml, 1.0 ml, 1.0 ml, and 1.0 ml of BAL fluid (0.9% saline with 0.6 mmol/L ethylenediaminetetraacetic acid warmed to 37°C) were instilled into the lungs. The fluid was allowed to sit for ~30 seconds before it was slowly removed from the lungs. The four aliquots were pooled for analysis. Cytospin slides were created using 150-μl aliquots and the Shandon Cytospin 3 centrifuge (Thermo Fisher Scientific, Inc., Waltham, MA). Manual cell counts and differentials were performed and confirmed that 97 to 99% of the BAL cells were macrophages.

Human Lung Tissue

Human lung tissue samples were obtained through the University of Pittsburgh Lung Tissue Center and were approved by University of Pittsburgh Institution Review Board. Sections of uninflated human lung tissue were mounted in O.C.T. compound and cryomolds were slowly frozen in liquid nitrogen. The specimens were stored at −80°C until needed. The frozen samples were cryosectioned to ~5 μm thickness.

Morphometry

Sample Preparation

Paraffin-embedded mouse lung sections were used for quantitative morphometric measurements. The paraffin was melted at 55°C for 20 minutes, and the slide was washed several times in xylene. The samples were rehydrated slowly in graded ethanol washes and then stained overnight in equal amounts of Gills solution (GHS-332; Sigma-Aldrich, St. Louis, MO) and Harris hematoxylin solution (HHS-32, Sigma-Aldrich). After several washes with water and ammonium hydroxide and with increasing concentrations of ethanol, the slides were allowed to air-dry.

Digital Imaging for Morphometric Measurements

After the coverslips were applied, digital images were obtained with the use of a light microscope (Zeiss Axiophot; Carl Zeiss MicroImaging, Thornwood, NY) equipped with a digital camera (Zeiss Axiocam HRc, Carl Zeiss MicroImaging). Twelve random images were taken at ×200 from seven smoke-exposed and five air-exposed animals and saved as tagged image file format (TIFF) images.

Mean Linear Intercept

Mean linear intercept measurements were taken using modified Image J software available from the National Institutes of Health website (*http://rsb.info.nih.gov/ij/*). Twelve black and white pictures for each animal were saved as 1300 × 1030 pixel digital images. Large airways, blood vessels, and other nonalveolar debris were manually removed from the image. The Image J software program automatically thresholded the images, and a median filter, set to a 2 pixel radius, smoothed the image edges. The program laid a line grid composed of 1353 lines (each line measuring 21 pixels) over the individual images. The software then counted the number of lines that ended on or intercepted alveolar tissue. These data were used to calculate the volume of air, the volume of tissue, the surface area, the surface area to tissue volume ratio. The mean linear intercept, which assesses the degree of alveolar airspace enlargement, was calculated using the equation: (4/surface area to volume tissue ratio) according to the methods adapted from Dunhill.[39] The mean linear intercept increases with increasing airspace enlargement.

Quantitative Morphometry of Airways

We examined airway thickening morphometrically based on our previously published methods[40] and those of George and colleagues[41] Briefly, paraffin-embedded lung sections prepared as described above were stained with hematoxylin and eosin. Airways were identified in sections at ×400, and images were captured digitally as described above. The analysis was performed with Metamorph Offline software, version 7.1.0.0 (Molecular Devices Corp., Sunnyvale, CA). Obliquely cut airways showing a length to width ratio >2.0 were excluded from analysis. Airways were divided into three groups based on diameter: 1) small airways 90 μm or less in diameter; 2) medium airways 90 to 129 μm in diameter; and 3) large airways >129 μm in diameter. Airway epithelial area and subepithelial area were calculated for each airway by defining the internal perimeter, external perimeter, and basement perimeter.

Immunofluorescence

Antibodies

Immunostaining was performed using rabbit polyclonal anti-CX3CR1, rabbit polyclonal anti-prosurfactant protein C (Abcam, Cambridge, MA); mouse monoclonal anti-CD68 (Santa Cruz Biotechnology, Inc., Santa Cruz, CA); rat anti-mouse MAC3 and Armenian hamster anti-mouse CD3ε (BD Biosciences Pharmingen, San Diego, CA); rat monoclonal anti-Gr1 (Cedarlane, Ontario, Canada); Armenian hamster anti-mouse CD11c (eBioscience, San Diego, CA); rat anti-mouse CD11b (clone M1/70.15; MorphoSys US Inc., Raleigh, NC). Immunostaining using control antibodies rabbit IgG, mouse IgG, rat IgG, and/or Armenian hamster IgG was performed on serial lung sections. Secondary antibodies to rabbit, goat, mouse, rat, and Armenian hamster were conjugated with Cy3 or Alexa488.

Immunofluorescence of Paraffin-Embedded Human and Murine Lung Sections

Paraffin-embedded sections were deparaffinized by warming the slides to 55°C on a slide warmer for 10 minutes and then washing the slides several times in xylene. Graded ethanol washes were used to rehydrate the samples, and the antigen retrieval step was performed by heating the samples on high in the microwave in an acidic citrate bath. Samples were blocked with 5% serum for 1 hour at room temperature. The primary antibody was allowed to incubate for 18 hours at 4°C. After several washes in PBS, the samples were incubated with the secondary antibody for 1 hour at room temperature. After several washes in PBS, Hoechst nucleic acid stain, diluted 1:1000 (Invitrogen Corp., Carlsbad, CA), was applied for 30 seconds. After several more washes in PBS, the samples were allowed to air-dry, and a coverslip was applied.

Immunofluorescence of Frozen Human and Murine Lung Sections

Frozen, O.C.T.-inflated samples were cut to 5-μm sections and fixed in acetone at −20°C for 2 minutes. After drying for 30 minutes at room temperature, the samples were rehydrated in a PBS wash. The blocking step and the incubation of the primary and secondary antibodies were completed as described for the paraffin-embedded samples.

Imaging

Immunofluorescence imaging was performed using an Olympus Provis Ax-70 microscope and digital camera (Olympus America, Center Valley, PA) with the assistance of MagnaFire 2.1B (Indigo Scientific, Ltd., Baldock, Hertfordshire, UK) imaging software. Images were acquired at ×400 in the individual red, blue, and green channels, and a color, 24-bit, merged TIFF image was created and saved for analysis. A minimum of 10 random images of alveolar tissue was acquired from each lung sample. If a random high-powered field contained large airways or blood vessels, the image was not captured and the next random field was examined.

Image Analysis and Quantitation of Immunostaining

The images of the alveolar parenchyma were analyzed using Metamorph Offline software, version 7.1.0.0 (Molecular Devices Corp.). Individual images for each lung sample were loaded into a single stack, and the color channels of the 24-bit TIFF images were separated. To normalize for the amount of lung tissue in a given high-powered field, the count nuclei application was used to quantify the total number of nuclei in the blue channel (Hoechst nucleic acid staining). The color images were converted into monochrome images, and the inclusive threshold tool was used to highlight the individual nuclei. The images were collectively thresholded as a stack. In some instances, in which the exposure times on the images had changed, the thresholding levels were adjusted. Cell counts of the various immune cells were performed by manual counting of cells immunostained with a given antibody. Each image was examined individually, and the number of positively staining immune cells was calculated as a percentage of total number of cells per high-power field.

Quantitative Reverse Transcriptase-Polymerase Chain Reaction (RT-PCR)

Our method of quantitative RT-PCR has been previously described.[33,38] Briefly, the left lung was homogenized, and RNA was extracted using the TRIzol method (Invitrogen Corp.). The RNA samples were reverse-transcribed into cDNA, which served as template for real-time PCR. Probes and primers for the tumor necrosis factor (TNF)-α, interferon-γ, CCL2, CX3CL1, CX3CR1, interleukin (IL)-6, matrix metalloproteinase (MMP)-7, MMP-9, and MMP-12 murine genes were commercially available, as was the TaqMan Master Mix containing the necessary reagents for gene expression studies (Applied Biosystems, Foster City, CA). Gene expression was analyzed by the ΔΔ-threshold cycle (ΔΔ-Ct) method, with 18S rRNA as the endogenous control, and average ΔCt of age-matched, gender-matched, air-exposed mice at the same time point serving as the calibrator.

Intratracheal Instillation of CX3CL1 and Lipopolysaccharide (LPS)

Male AKR/J mice (The Jackson Laboratory) mice were anesthetized using a mixture of isoflurane and oxygen bled in at 3 L/minute. We instilled PBS plus 0.1% nonpyrogenic human serum albumin, 10^{-6} mol/L CX3CL1 (R&D Systems, Minneapolis, MN) diluted in PBS plus 0.1% human serum albumin, or 10^{-6} mol/L CX3CL1 and 0.5 mg/ml LPS (List Biological Laborato-

ries, Inc., Campbell, CA) in PBS and 0.1% human serum albumin intratracheally using direct laryngoscopy to visualize the airway. The volume of instillate was determined according to the weight of the animal using the formula: (150 μl/100 g mouse)(X g mouse) = Y μl instillate. After intratracheal instillation, the animals were allowed to recover in the surgical area. After 24 hours, the animals were sacrificed with an intraperitoneal injection of pentobarbital as described above. The trachea was cannulated, and whole lung lavage was performed as described above.

Cytospin slides were created using 150-μl aliquots as noted above in the Materials and Methods under BAL. Manual cell counts and differentials were performed. The remaining slides were fixed in 100% acetone for 3 minutes and then stored at −80°C. Immunostaining was performed on the fixed cytospin slides using the rabbit polyclonal anti-CX3CR1 antibody and immunofluorescence protocol as described above.

Immunofluorescence Labeling of RAW264.7 Cells after Stimulation with LPS

RAW264.7 mouse macrophage-like cells were grown in medium containing Dulbecco's modified Eagle's medium with 10% fetal bovine serum, 100 U/ml penicillin, and 0.1 mg/ml streptomycin. On day 0, RAW264.7 cells were added to the media, seeded onto glass chamber slides, and grown overnight at 37°C. Increasing concentrations of LPS (0 ng/ml, 1 ng/ml, 10 ng/ml, and 100 ng/ml) were added to the appropriate chambers, and the cells were returned to the 37°C incubator for 24 hours. The cells were washed with 0.5% bovine serum albumin in PBS several times, fixed in 4% paraformaldehyde in PBS for 15 minutes on ice, and permeabilized with 0.1% Triton X (Sigma-Aldrich, St. Louis, MO) on ice. After several more washes with 0.5% bovine serum albumin in PBS, the cells were blocked in 2% bovine serum albumin for 20 minutes at room temperature. Rabbit anti-human CX3CR1 antibody and a nuclear marker, DRAQ5 (Biostatus Limited, Shepshed, Leicestershire, UK), or a rabbit IgG antibody control and DRAQ5 were allowed to incubate for 60 minutes at room temperature. After several washes with 0.5% bovine serum albumin in PBS, the cells were incubated with the secondary antibody for 30 minutes at room temperature. After several washes, a coverslip was applied. Immunofluorescence imaging was performed as described above.

Statistical Analysis

The experimental data are expressed as the mean ± the SEM. Statistical analysis was done using one-way analysis of variance for pairwise multiple comparisons. If the data failed the test for normality, statistical analysis was completed using Kruskal-Wallis one-way analysis of variance on ranks and pairwise multiple comparison procedures performed. For serial measurements, we used analysis of variance repeated measurements. A P value <0.05 was considered significant. All statistics were run on SigmaStat software version 3.5 (Systat Software, Inc., San Jose, CA).

Results

Chronic Cigarette Smoke Exposure Results in Airspace Enlargement, Failure to Thrive, and Inflammatory Cell Recruitment into the Lungs

AKR/J mice were used for this study because this mouse strain has been shown to have a significant inflammatory response and increased susceptibility to chronic cigarette smoke-induced emphysema.[42] Mice that underwent chronic environmental tobacco smoke exposure showed an increase in airspace enlargement by 24 weeks (Figure 1, A and B), as evidenced by an increase in mean linear intercept when compared to the air-exposed controls (Figure 1C; Lm 31.75 μm versus 29.54 μm, $P = 0.014$). Although Guerassimov and colleagues[42] observed a 38% increase in airspace enlargement in the same strain using the direct nose-cone approach to delivering cigarette smoke, the modest increase in airspace enlargement above air-exposed mice we observed more closely reflects other wild-type strains exposed to environmental tobacco smoke using the total body exposure method.[34] The increase in airspace enlargement in the cigarette smoke-exposed mice, corresponding to the degree of alveolar tissue destruction or emphysema, was also associated with systemic effects. Although the air-exposed mice steadily gained weight and averaged 46.2 g after 24 weeks, the cigarette smoke-exposed mice did not lose or gain a significant

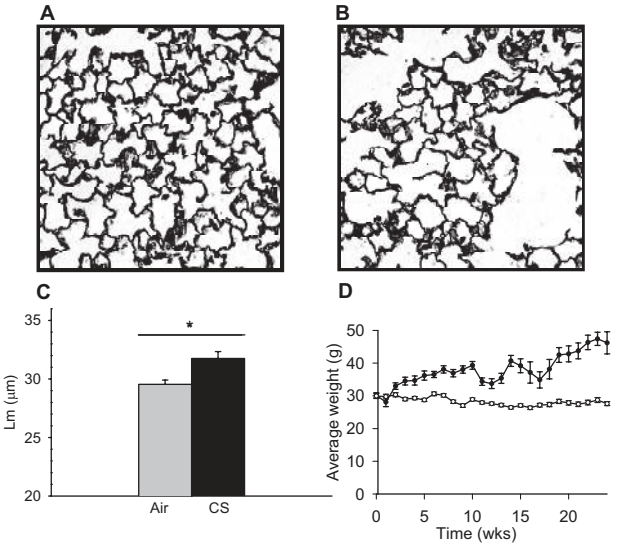

Figure 1. Histological and systemic changes attributable to chronic cigarette smoke exposure. **A** and **B:** Representative images of mouse lungs after 24 weeks of air (**A**) or cigarette smoke exposure (**B**). The samples were stained using the modified Gills technique. **C:** Environmental tobacco smoke exposure is associated with an increase in airspace enlargement by 24 weeks. There is an increase in mean linear intercept (Lm) measured after 24 weeks in the cigarette smoke (CS)-exposed mice (31.75 μm) when compared to the air-exposed controls (29.54 μm). *$P = 0.014$, $n = 5$ to 7 mice per group. **D:** The average weights of the cigarette smoke-exposed mice (**white circles**) were significantly lower than the average weights of the air-exposed mice (**black circles**), $P < 0.001$ (analysis of variance repeated measurements). The smoke- and air-exposed mice averaged 30.0 g at t = 0. The air-exposed mice steadily gained weight and averaged 46.2 g after 24 weeks. The smoke-exposed mice did not lose or gain a significant amount of weight and averaged 27.6 g after 24 weeks. Error bars at each time point indicate ±SEM $n = 12$ mice in each group for exposures up to 12 weeks. $n = 7$ mice in each group for exposures from 13 to 24 weeks. Original magnifications, ×200.

Table 1. Cellular Inflammatory Response after 12 and 24 Weeks of Chronic Cigarette Smoke or Air Exposure

	12 Weeks air	12 Weeks cigarette	24 Weeks air	24 Weeks cigarette
% Macrophages*	5.0 ± 1.1	7.3 ± 1.9	2.9 ± 0.3	5.6 ± 0.6‡
Total cells/hpf†	320 ± 10	296 ± 13	340 ± 8	230 ± 7‡§
% $CD3^+$ cells*	5.8 ± 0.3	7.2 ± 0.5¶	7.2 ± 0.4	8.3 ± 0.5
Total cells/hpf†	325 ± 9.5	306 ± 10.7	265 ± 7.3‖	225 ± 6.4‡§
% GR-1^+ cells*	0.4 ± 0.1	0.2 ± 0.0	1.5 ± 0.2	1.9 ± 0.3
Total cells/hpf†	315 ± 5.5	307 ± 13	275 ± 8.5	232 ± 8.2‡§

n = 50 random high-powered fields (hpf) of alveolar parenchymal tissue examined from five animals per condition at 12 weeks, n = 20 random high-powered fields examined from five animals per condition at 24 weeks.
*Immune cells expressed as mean percentage of total cells per hpf ± SE.
†Total number of cells counted per hpf with values expressed as mean ± SE.
‡Twenty-four weeks of air versus 24 weeks of cigarette smoke exposure, $P < 0.001$.
§Twelve weeks of air or cigarette exposure versus 24 weeks of cigarette smoke exposure, $P < 0.001$.
¶Twelve weeks of air versus 12 weeks of cigarette smoke exposure, $P = 0.04$.
‖Twelve weeks of air versus 24 of weeks air exposure, $P < 0.001$.

amount of weight and averaged 27.6 g after 24 weeks ($P < 0.001$, Figure 1D). We also examined airway wall thickening morphometrically based on our previous published methods[40] and those of George and colleagues[41] after 6 months of exposure. We did not observe significant differences in subepithelial airway wall thickening between air- and cigarette-exposed mice in small airways (90 μm or less in diameter, $P = 0.6$), medium-sized airways (90 to 129 μm in diameter, $P = 0.4$), and large airways (>129 μm in diameter, $P = 0.9$) (data not shown).

The local inflammatory response was characterized by an increase in the percentage of macrophages in cigarette smoke-exposed mice at 12 weeks compared to air-exposed controls (7.3% versus 5.0%, $P = 0.07$) that reached significance by 24 weeks (5.6% versus 2.9%, $P < 0.001$) (Table 1). There was an increase in the percentage of $CD3^+$ cells in smoke-exposed mice at 12 weeks compared to air-exposed controls (7.2% versus 5.8%, $P = 0.04$), but the difference was not significant by 24 weeks (8.3% versus 7.2%, $P = 0.12$). There was an increase in the percentage of polymorphonuclear cells in cigarette smoke-exposed mice by 24 weeks when compared to air-exposed controls, but this was not significant (1.9% versus 1.5% at 24 weeks, $P = 0.26$). Thus, chronic cigarette smoke exposure is associated with an increased recruitment of immune cells in the lung parenchyma comprised of macrophages, T lymphocytes, and polymorphonuclear cells with the most notable increases in the macrophage and T-lymphocyte populations.

Interestingly, total numbers of cells comprising the lung parenchyma per high-powered field was reduced with increasing duration of exposure (Table 1). The greatest reduction in numbers observed was in mice exposed to 24 weeks of cigarette smoke compared with either 12 weeks of air exposure ($P < 0.001$), 12 weeks of cigarette smoke exposure ($P < 0.001$), or 24 weeks of air exposure ($P < 0.001$). The reduced cellularity in alveolar tissue is consistent with airspace enlargement and lung parenchymal destruction that characterizes cigarette smoke-induced emphysema. In air-exposed mice, this pattern of reduced cellular numbers was less consistent. This may reflect the effects of aging on airspace enlargement that occurs both in humans and in mice.[43,44]

Accumulation of $CX3CR1^+$ Cells in the Lungs after Chronic Cigarette Smoke Exposure

CX3CR1 protein expression was detectable in the lung parenchyma of unstimulated mice (Figure 2A) and increased significantly after chronic cigarette smoke exposure (Figure 2B). CX3CR1 localized to mononuclear cells of both the interstitium and alveolar spaces (Figure 2, A and B).

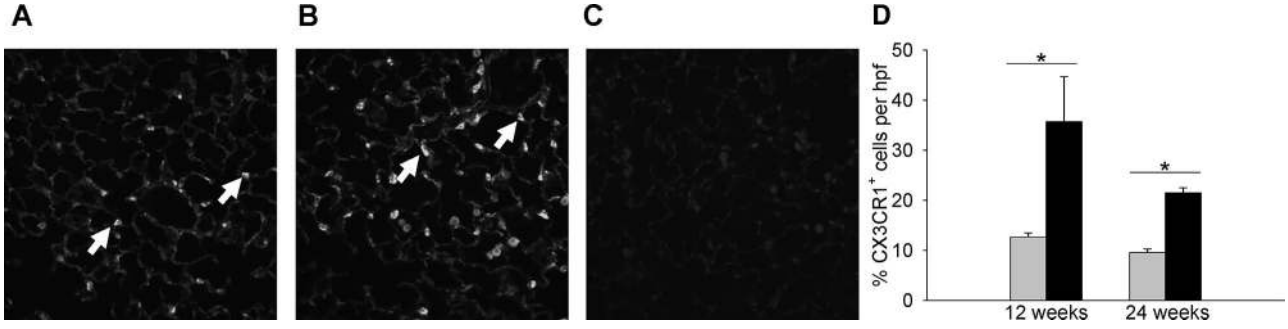

Figure 2. $CX3CR1^+$ cells in the lungs of chronic cigarette smoke-exposed mice and air-exposed controls. **A** and **B:** Representative images used for the quantitation of $CX3CR1^+$ cells in mouse lungs after 12 weeks of either air exposure (**A**) or cigarette smoke exposure (**B**). The **arrows** indicate CX3CR1 immunostaining of discrete, mononuclear cells within the parenchyma. **C:** Rabbit IgG control immunostaining of murine lung section after 12-week cigarette smoke exposure. **D:** $CX3CR1^+$ cells as a percentage of total cells per high-powered field in lung sections from air-exposed controls and cigarette-exposed mice after 12 weeks (12.7 ± 0.8 versus 35.7 ± 9) and 24 weeks (9.6 ± 0.7 versus 21.5 ± 1) of exposure. *$P < 0.001$. Gray bars, air-exposed controls; black bars, cigarette smoke-exposed group. n = 50 random hpf of lung parenchymal sections examined from five animals per condition at 12 weeks, n = 20 random hpf examined from five animals per condition at 24 weeks. Original magnifications, ×400.

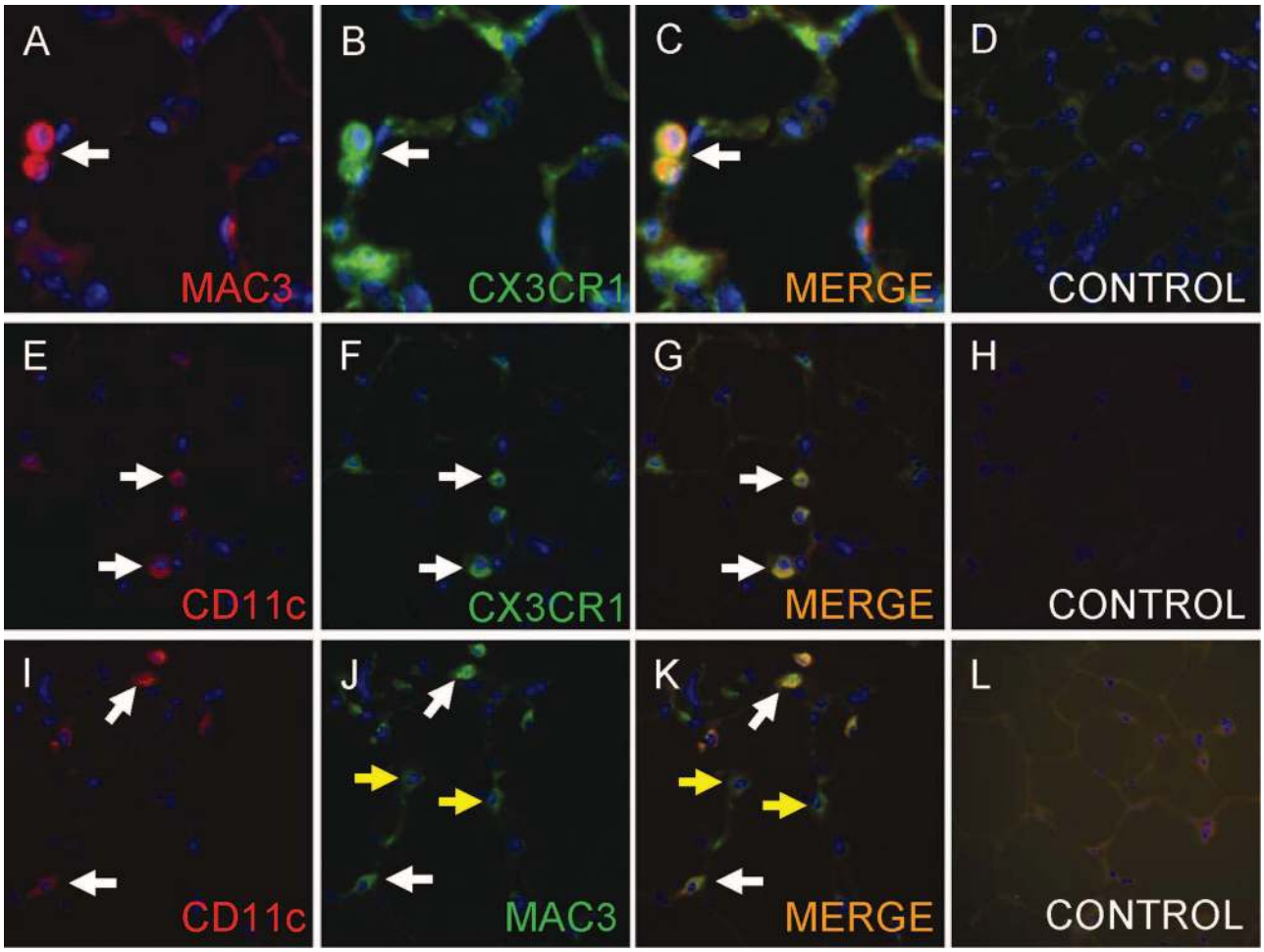

Figure 3. MAC3$^+$, CX3CR1$^+$, and CD11c$^+$ cells in murine lungs after cigarette smoke exposure. **A:** MAC3 immunostaining (red channel). **B:** CX3CR1 immunostaining (green channel). **C:** Co-localization of MAC3 and CX3CR1 (merged channels); **white arrows**. **D:** Absence of immunostaining in studies using rat and rabbit IgG control antibodies. **E:** CD11c immunostaining (red channel). **F:** CX3CR1 immunostaining (green channel). **G: White arrows** indicate cells that co-localize with CD11c and CX3CR1 (merged channels). **H:** Absence of immunostaining in studies using Armenian hamster IgG and rabbit IgG control antibodies. **I:** CD11c expression (red channel). **J:** MAC3 expression (green channel). **K:** Co-localization of CD11c and MAC3 (**white arrows**, merged channels). **Yellow arrows** indicate cells that express MAC3 (green) but do not express CD11c. **L:** Absence of immunostaining in studies using Armenian hamster IgG and rat IgG control antibodies. Original magnifications, ×400.

Quantitative analysis revealed an increase in the percentage of CX3CR1$^+$ cells per total number of cells counted under high-powered field in cigarette smoke-exposed mice when compared to the age-matched air-exposed controls after 12 weeks (35.7% versus 12.7%, $P < 0.001$) (Figure 2D). This difference was sustained to 24 weeks of exposure (21.5% versus 9.6%, $P < 0.001$) (Figure 2D).

CX3CR1 Is Expressed by Mononuclear Phagocytes in the Lungs

We immunophenotyped cells expressing CX3CR1 in mice after chronic cigarette smoke exposure. CX3CR1 co-localized to cells expressing the macrophage surface antigen, MAC3 (Figure 3, A–C). Both macrophages and dendritic cells express the β-integrin, CD11c,[45] and, consistent with findings of others,[45,46] CD11c$^+$ cells also express CX3CR1 in our experimental model (Figure 3, E–G). CD11c$^+$ cells within the lung parenchyma were macrophage in origin, as evidenced by co-expression of the MAC3 surface antigen (Figure 3, I–K; white arrows). Although two populations of macrophages emerged based on the presence or absence of CD11c expression (Figure 3K; white and yellow arrows, respectively), CX3CR1 expression did not appear to distinguish between the two (data not shown). Given prior reports that CX3CR1 is expressed on lung dendritic cells but not pulmonary macrophages,[45] we also immunostained for CX3CR1 expression in human lung samples and found many mononuclear cells expressing CX3CR1 (Figure 4). These mononuclear cells expressed both CX3CR1 and the macrophage marker CD68 (Figure 4, A–C). Thus, our findings confirm that both mouse and human pulmonary macrophages express CX3CR1.

CX3CR1 Is Expressed by CD3$^+$ Cells but Not Neutrophils or Type II Pneumocytes in the Lungs

The percentage of CD3$^+$ T lymphocytes per total numbers of cells in the lung parenchyma increased with

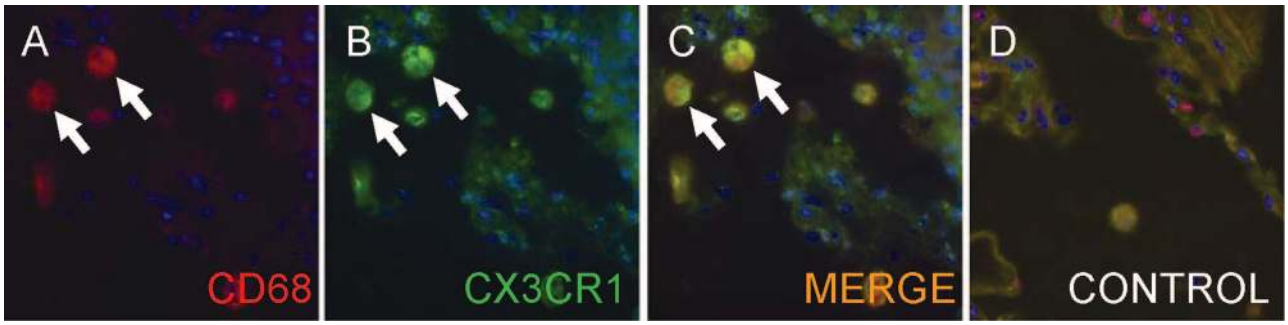

Figure 4. CD68$^+$ human alveolar macrophages express CX3CR1. **A:** CD68 immunostaining identifies macrophages in human lung tissue (**white arrows**, red channel) (uninflated lung sections from human explants). **B:** CX3CR1 immunostaining (**white arrows**, green channel). **C:** Co-localization of CX3CR1 and CD68 on human alveolar macrophages (**white arrows**, merged channels). **D:** Absence of immunostaining in studies using rabbit IgG and mouse IgG control antibodies. Original magnifications, ×400.

chronic cigarette smoke exposure (Table 1). We show that CX3CR1 also co-localized to cells expressing the CD3 antigen (Figure 5, A–C) in murine lung parenchyma. In contrast, CX3CR1 was not expressed on neutrophils (Figure 5, E–G; white arrow). We also assessed whether type II pneumocytes express CX3CR1. Because antibodies to prosurfactant protein C (pro-SPC), a type II pneumocyte marker, and CX3CR1 were both derived from a rabbit host making co-localization studies unreliable, we examined type II pneumocytes from B6.129P-*cx3cr1*^{tm1Litt}/J mice with enhanced green fluorescent protein (EGFP) at the *cx3cr1* loci. Prosurfactant protein C did not co-localize with EGFP, suggesting that cells comprising the alveolar architecture do not express CX3CR1 constitutively (Figure 5, I–K; white arrows). Furthermore, immunofluorescence studies using serial lung sections from AKR/J mice confirmed that chronic cigarette smoke exposure did not induce CX3CR1 protein expression on type II pneumocytes (Figure 5, L and M).

Up-Regulation of CX3CL1 Gene Expression Characterizes the Lung Tissue and Alveolar Macrophage Inflammatory Response

TNF-α, IL-6, and CX3CL1 gene expression were increased in lung tissue homogenates from cigarette smoke-exposed mice when compared to air-exposed controls after 12 weeks of exposure ($P \leq 0.03$, Figure 6A). However, there was no difference in CX3CR1, CCL2, and interferon-γ gene expression between cigarette smoke- and air-exposed mice (Figure 6A). By 24 weeks, CX3CL1 gene expression remained increased fivefold in lung tissue from cigarette smoke-exposed mice as compared to age-matched air-exposed controls ($P = 0.03$, Figure 6B). CX3CR1 gene expression doubled in the lung tissue of cigarette smoke-exposed mice after 24 weeks of chronic smoke exposure, but the difference compared to air-exposed controls was not significant ($P = 0.14$, Figure 6B). Thus, CX3CL1 gene expression is up-regulated in lung tissue after chronic cigarette smoke exposure. The failure to detect a clear CX3CR1 signal in homogenates might very well reflect a dilutional effect of including combined cell populations because the homogenized lung tissue represents the intravascular, parenchymal, alveolar, and airway compartments.

Macrophages, the cellular type that makes up the majority of cells in BAL, are believed to play an important role in the chronic inflammatory process of cigarette smoke-exposed lungs that results in emphysema and COPD.[47–49] We examined the gene expression of BAL cells after 12 weeks of exposure, the time point at which we observed maximal differences in gene expression in the lung homogenates. We found a 10-fold increase in CX3CL1 and CX3CR1 expression and $>$ 20-fold increase in CCL2, IL-6, and TNF-α when compared to air-exposed controls ($P \leq 0.008$, Figure 6C). Interestingly, chronic cigarette smoke exposure did not up-regulate interferon-γ gene expression in BAL cells, the majority of which was comprised of alveolar macrophages (97 to 99% of the total cells counted in prepared cytospins) (Figure 6C). However, both CX3CL1 and CX3CR1 gene expression characterized the inflammatory gene expression profile of alveolar macrophages in response to chronic cigarette smoke exposure.

As supporting evidence for activated macrophage-induced parenchymal lung tissue destruction, we also examined metalloproteinase gene expression in lung tissue homogenates at the 12- and 24-week time point. There were no significant differences in MMP-7, MMP-9, and MMP-12 gene expression at the 12-week time point (data not shown). By 24 weeks, MMP-12, but not MMP-7 or MMP-9, gene expression was up-regulated in cigarette-exposed mice compared with air-exposed controls ($P = 0.006$, Figure 6D).

LPS-Induced Inflammation Increases CX3CR1 Expression on RAW264.7 Cells and Alveolar Mononuclear Phagocytes

Given the sustained accumulation of CX3CR1$^+$ cells in the lungs and the inducibility of its expression in alveolar macrophages after chronic cigarette smoke, we investigated the inducibility of CX3CR1 expression using an acute inflammatory stimulus such as LPS in RAW264.7 cells, a mouse macrophage-like cell line, *in vitro*. RAW264.7

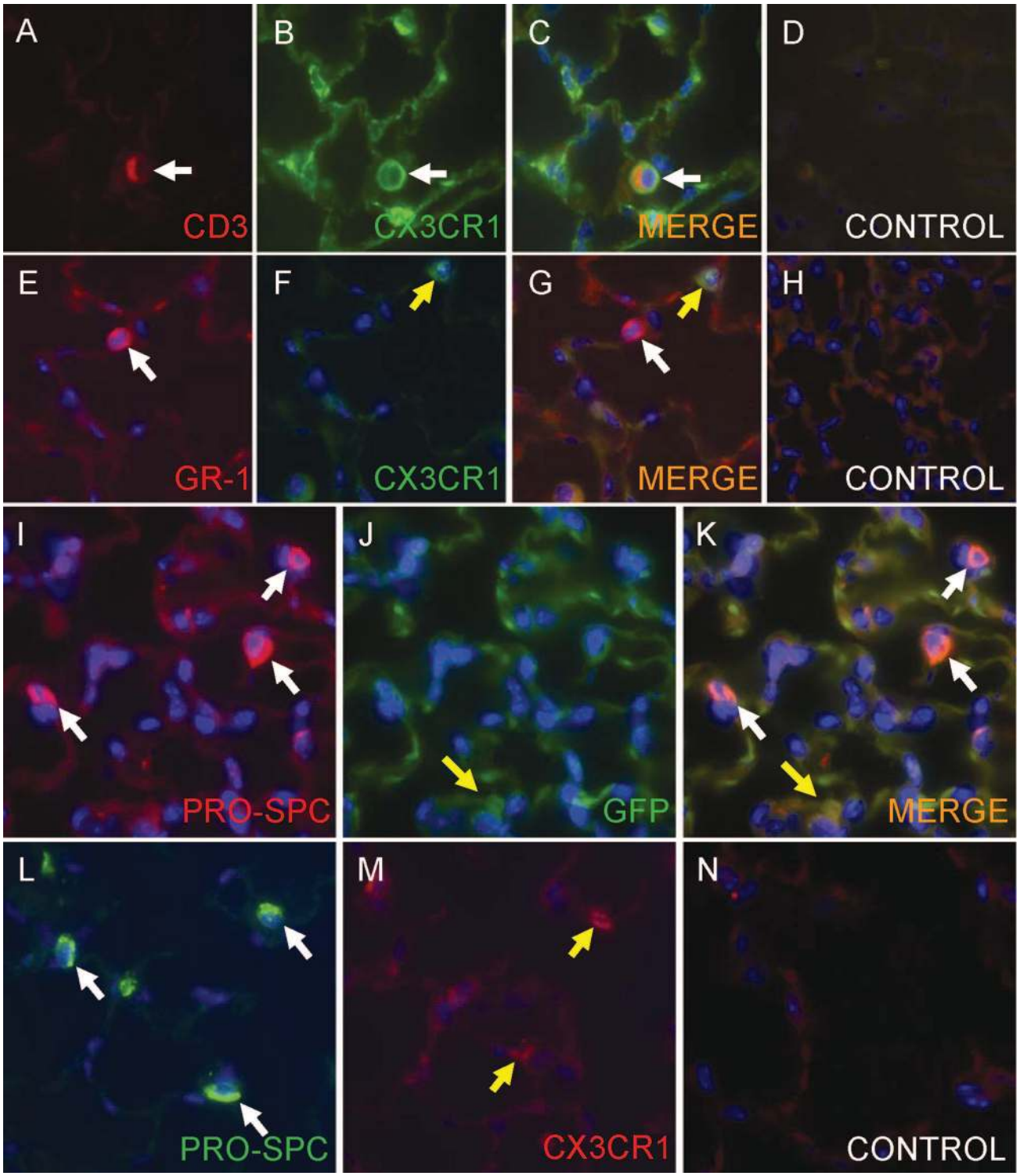

Figure 5. CD3^{+} cells but not Gr-1^{+} or pro-SPC^{+} cells express CX3CR1 in murine lungs. **A:** CD3 immunostaining (red channel). **B:** CX3CR1 immunostaining (green channel). **C:** Co-localization of CD3 and CX3CR1 in cell with eccentric nucleus (merged channels). **D:** Absence of immunostaining in studies using Armenian hamster IgG and rabbit IgG control antibodies. **E:** Gr-1^{+} immunostaining (red channel). **F:** CX3CR1 immunostaining (green channel). **G: White arrow** indicates polymorphonuclear cell is Gr-1^{+} but CX3CR1^{-}, and **yellow arrow** indicates mononuclear cell is CX3CR1^{+} but Gr-1^{-} (merged channels). **H:** Absence of immunostaining in studies using rat IgG and rabbit IgG control antibodies. **I:** Pro-SPC immunostaining (red channel) in unstimulated B6.129P-*cx3cr1*^{tm1Litt}/J mouse lung. **J:** GFP signal (**yellow arrow**) indicating endogenous CX3CR1 expression (green channel). **K: Yellow arrow** indicates cell that is CX3CR1^{+} but pro-SPC^{-}, and **white arrows** indicate cells that are pro-SPC^{+} but CX3CR1^{-} (merged channels). **L** and **M:** Serial sections from AKR/J mouse lungs after 12 weeks of cigarette smoke exposure confirm that pro-SPC^{+} cells are discrete from CX3CR1^{+} cells. **White arrows** indicate pro-SPC^{+} cells (**L**, green channel). **Yellow arrows** indicate CX3CR1^{+} cells (**M**, red channel). **N:** Absence of immunostaining in studies using rabbit IgG control antibody. Original magnifications, ×400.

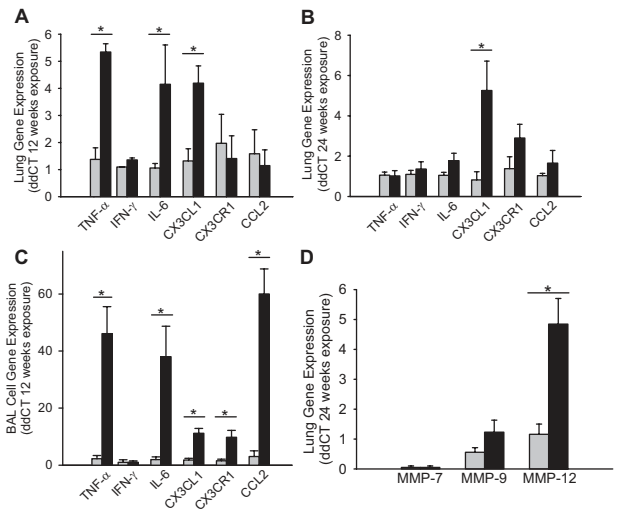

Figure 6. Relative gene expression in lung tissue homogenates and BAL cells of mice after chronic air or cigarette smoke exposure. **A:** Relative gene expression in lung tissue homogenates from air-exposed mice (gray bar) compared to cigarette smoke-exposed mice (black bar) shows up-regulation of TNF-α, IL-6, and CX3CL1 after 12 weeks of cigarette smoke exposure. $^*P \leq 0.03$. **B:** Relative gene expression in lung tissue homogenates after 24 weeks of cigarette smoke exposure shows CX3CL1 up-regulated compared to air-exposed controls. $^*P = 0.03$. **C:** The relative gene expression in BAL cells from air-exposed mice (gray bar) compared to cigarette smoke-exposed mice (black bar) demonstrates increase in TNF-α, IL-6, CX3CL1, CX3CR1, and CCL2 after 12 weeks of cigarette smoke exposure. $^*P \leq 0.008$. **D:** Relative gene expression of metalloproteinase (MMP)-7, -9, and -12 in lung tissue homogenates after 24 weeks of cigarette smoke exposure. MMP-12 gene expression was up-regulated with cigarette smoke exposure when compared to air-exposed controls. $^*P = 0.006$. Gene expression was analyzed by the ΔΔ-threshold cycle (ΔΔ-Ct) method, with 18S rRNA as the endogenous control. The average ΔCt of age-matched, gender-matched, air-exposed mouse samples served as the calibrator. Gray bars represent air-exposed lungs. Black bars represent cigarette smoke-exposed lungs. $n = 3$ to 5 mice in each group for 12-week lung homogenate data; $n = 5$ to 7 mice for 12-week BAL and 24-week lung homogenate data.

cells expressed CX3CR1 at baseline (Figure 7B). Increasing concentrations of LPS enhanced CX3CR1 expression in RAW264.7 cells *in vitro* (Figure 7, B–D) in a dose-dependent manner. We also examined the inducibility of CX3CR1 expression in alveolar mononuclear phagocytes *in vivo*. Intratracheal administration of CX3CL1 ligand alone only mildly increased CX3CR1 expression in murine alveolar mononuclear phagocytes from baseline (Figure 7G). However, the combined instillation of CX3CL1 and LPS considerably enhanced CX3CR1 expression (Figure 7H). The enhanced CX3CR1 expression in alveolar mononuclear phagocytes was associated with fivefold up-regulation of CX3CR1 gene expression in BAL cells (data not shown). Thus, acute inflammatory stimulus, such as LPS, increases CX3CR1 expression in mononuclear phagocytes both *in vitro* and *in vivo*.

Discussion

Comprehensive gene expression profiling has previously identified up-regulation of the chemokine CX3CL1 in human lungs with COPD.[17] Whether or not increases in CX3CL1 gene expression are associated with the recruitment and amplification of $CX3CR1^+$ cells in the lungs is not known. In this study, we examined for the presence of CX3CR1 in the lungs during chronic cigarette smoke-induced emphysema. Mice exposed to cigarette smoke showed accumulation of $CX3CR1^+$ cells within the lung parenchyma that was sustained at 24 weeks of exposure and was associated with the development of air space enlargement and parenchymal tissue loss, the histological hallmarks of emphysema. The increase in $CX3CR1^+$ cells was primarily comprised of mononuclear phagocytes and T lymphocytes, two cell populations implicated in the pathogenesis of cigarette smoke-induced emphysema.[5,6,16]

In our study, we show increased CX3CL1 gene expression in murine lungs after prolonged cigarette smoke exposure. In alveolar macrophages, cigarette smoke exposure increased both CX3CR1 and CX3CL1 gene expression, suggesting a mechanism whereby macrophages amplify and sustain CX3CR1 cells within the lungs during chronic inflammation. The inducibility of CX3CR1 expression was not solely dependent on a chronic stimulus because LPS also increased CX3CR1 expression in RAW264.7 cells *in vitro* and in alveolar mononuclear phagocytes *in vivo*. Others have previously reported that CX3CL1 provides cell-survival signals on ligation of CX3CR1[50,51] and inhibits Fas-mediated apoptosis in microglial cells.[52] Whether or not the CX3CL1-CX3CR1 pathway promotes cell-survival signals and contributes to the accumulation of alveolar and parenchymal macrophages observed in COPD is not known.

Fogg and colleagues[46] have recently shown that a clonogenic bone marrow progenitor cell expressing CX3CR1 can give rise to monocytes, macrophages, and dendritic cells. They suggest that the macrophage and dendritic cell precursor (MDP), in the setting of specific stimulating factors and chemokines, can generate inflammatory dendritic cells and macrophages, resident macrophages, and resident $CD11c^+$ dendritic cells. Furthermore, Geissman and colleagues[53] proposed two functional subsets of murine blood monocytes. One subset, $CX3CR1^{lo}Gr1^+$, is recruited to inflamed tissue where it differentiates into dendritic cells and triggers naïve T-lymphocyte proliferation. A second subset is identified as $CX3CR1^{high}Gr1^-$ cells, and is dependent on CX3CR1-CX3CL1 interactions to enter noninflamed tissues. Although their experimental system examined monocyte differentiation properties after an acute inflammatory stimulus elicited by intraperitoneal thioglycollate injection, the lungs as a comparator showed recruitment of predominantly $CX3CR1^{high}Gr1^-$ monocytes. These $CX3CR1^{high}Gr1^-$ monocytes serve as a precursor for resident myeloid cells and have the capacity to differentiate into dendritic cells.

In our model of chronic cigarette smoke-induced inflammation, the lungs demonstrated increased recruitment of $CX3CR1^+$ cells of macrophage lineage. Others have previously shown that alveolar and lung tissue macrophages exhibit high autofluorescence, in contrast to dendritic cells.[54,55] We have also noted this property of macrophages by fluorescence microscopy. In addition, the MAC3 antigen is a commonly used marker for macrophages, both by flow cytometry[56] and by immunohistochemical technique.[57] It has been suggested by others

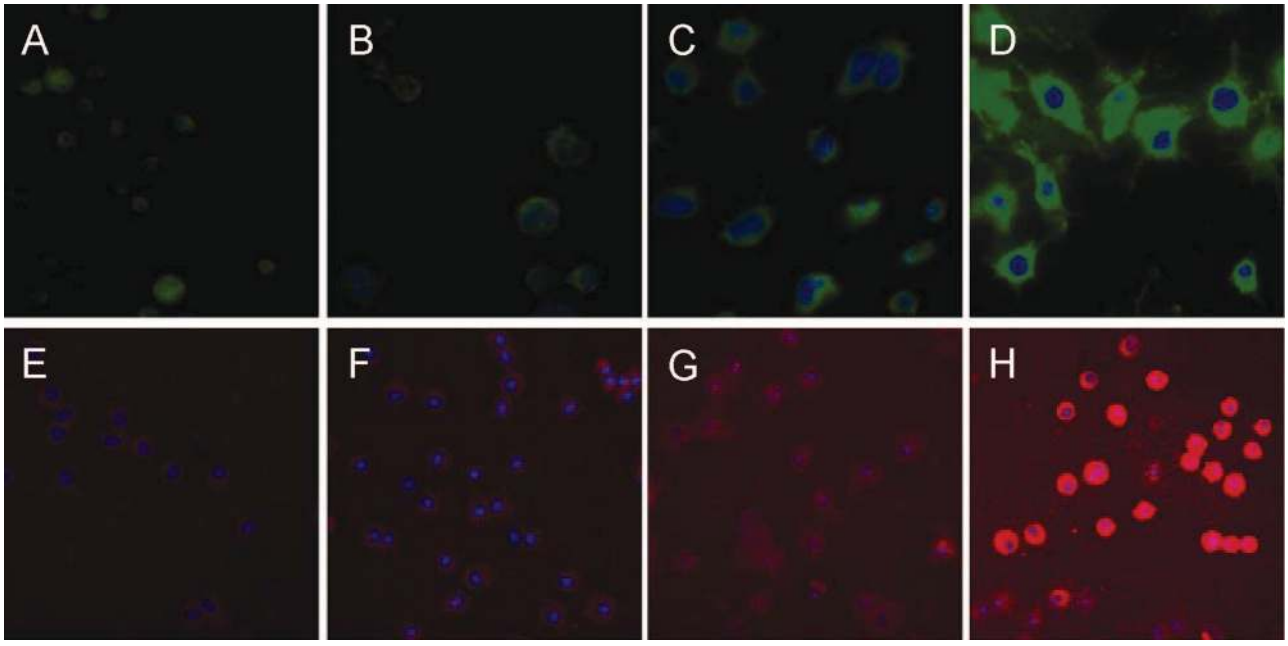

Figure 7. LPS induces CX3CR1 expression in RAW264.7 cells *in vitro* and in alveolar mononuclear phagocytes *in vivo*. **A:** Absence of immunostaining in RAW264.7 cells using rabbit IgG control antibody. **B:** CX3CR1 expression in unstimulated RAW264.7 cells. **C:** CX3CR1 expression in RAW264.7 cells after 24 hours of stimulation with LPS (10 ng/ml). **D:** CX3CR1 expression in RAW264.7 cells after 24 hours of stimulation with LPS (100 ng/ml). **E–H:** CX3CR1 expression in mononuclear phagocytes from BAL 24 hours after intratracheal instillation of stimulus. **E:** Absence of immunostaining with rabbit IgG control antibody. **F:** CX3CR1 expression after intratracheal instillation of PBS. **G:** CX3CR1 expression, after intratracheal instillation of CX3CL1 (1 μmol/L). **H:** CX3CR1 expression, after intratracheal instillation of CX3CL1 (1 μmol/L) + LPS (0.5 mg/ml). $N = 3$ to 7 mice in each group, two independent experiments. Original magnifications, $\times$100.

that CX3CR1 is a reliable marker for lung dendritic cells and that lung macrophages do not express CX3CR1.[45] In contrast to previous findings, we show that macrophages, distinguished from monocytes and dendritic cells by their autofluorescent property and the expression of the MAC3 antigen, are CX3CR1$^+$ *in vivo*.

Furthermore, Grayson and colleagues[56] found that MAC3$^+$/CD11c$^+$ cells in the lungs represent alveolar macrophages that exhibit distinct scatter characteristics from MAC3$^+$/CD11c$^-$ cells that represent tissue macrophages. Our findings show that both alveolar macrophages (MAC3$^+$/CD11c$^+$) and tissue macrophages (MAC3$^+$/CD11c$^-$) expressed CX3CR1 in the lungs. The findings in our mouse model of chronic cigarette smoke exposure are also supported by our findings in macrophages from human lung tissue and from RAW264.7 cells, which both express CX3CR1.

Although macrophages orchestrate local inflammatory processes and proteolytic destruction in lung tissue elicited by exposure to chronic cigarette smoke,[6] evidence also supports a role for T lymphocytes in the destruction of lung parenchyma in the setting of COPD and emphysema.[9] Finkelstein and colleagues[5] demonstrated a correlation between the number of alveolar macrophages and T lymphocytes in the lung and the severity of emphysema. We also show increased numbers of T lymphocytes in the lung parenchyma of these mice after chronic cigarette smoke exposure, and that the T lymphocytes are CX3CR1$^+$. CX3CR1$^+$ T lymphocytes represent differentiated effector cells that are ready to migrate into areas with active inflammation. Recent findings also suggest that Th1 lymphocytes expressing CCR5 and CXCR3 are preferentially recruited to the lungs in emphysema and facilitate proteolytic damage by up-regulating macrophage elastase expression.[16] This finding is intriguing because CX3CL1 can provide an amplification circuit of polarized type I responses.[58]

Our findings suggest that other cell populations express CX3CR1 in the lung parenchyma and are increased after chronic cigarette smoke exposure. Monocytes, precursors to resident macrophages, likely comprise a significant population of CX3CR1$^+$ cells that express neither macrophage nor T cell markers. It is possible that CD11c$^+$ MAC3$^-$ cells express CX3CR1, but this population was sparsely present in the lung sections examined. Given the paucity of optimal reagents, our study was not able to determine whether CX3CR1 cell populations in the lungs of AKR/J mice include NK cells.

In summary, we have shown that cigarette-induced emphysema is associated with recruitment and accumulation of CX3CR1$^+$ cells in the lungs. Immunophenotyping shows that T lymphocytes and tissue and alveolar macrophages, but not type II pneumocytes or neutrophils, express CX3CR1. We also show up-regulation of CX3CL1 gene expression in mice that develop emphysema. This up-regulation is temporally associated with an increase in CX3CR1$^+$ cells that is sustained after 24 weeks of chronic cigarette smoke exposure. Furthermore, cigarette smoke up-regulates CX3CL1 and CX3CR1 expression in alveolar mononuclear phagocytes *in vivo*. Our data also shows that even an acute inflammatory stimulus such as LPS can up-regulate CX3CR1 expression in macrophages, suggesting a mechanism by which macrophage accumulation is sustained and amplified during inflammatory conditions. The fact that LPS can also up-regulate CX3CR1 expression in macro-

phages is important because increasing evidence supports the theory of bacterial pathogens or colonizers of the lower respiratory tract as amplifiers or modulators of the host inflammatory response to chronic cigarette smoke exposure.[59] Finally, CX3CR1 readily identifies macrophages in human lungs, supporting a similar pattern of lineage commitment as observed in mice. The CX3CR1-CX3CL1 interaction plays an important role in the recruitment and activation of the mononuclear phagocyte system. It also mediates the rapid arrest and adhesion of T lymphocytes to endothelial cells in the setting of inflammatory stimuli. Our findings suggest that the CX3CR1-CX3CL1 pathway may be a common signaling pathway to recruit and amplify divergent immune cell populations in cigarette smoke-induced inflammation.

References

1. MacKenzie TD, Bartecchi CE, Schrier RW: The human costs of tobacco use (2). N Engl J Med 1994, 330:975–980
2. Murray CJ, Lopez AD: Alternative projections of mortality and disability by cause 1990–2020: Global Burden of Disease Study. Lancet 1997, 349:1498–1504
3. Hogg JC, Chu F, Utokaparch S, Woods R, Elliott WM, Buzatu L, Cherniack RM, Rogers RM, Sciurba FC, Coxson HO, Pare PD: The nature of small-airway obstruction in chronic obstructive pulmonary disease. N Engl J Med 2004, 350:2645–2653
4. Shapiro SD, Ingenito EP: The pathogenesis of chronic obstructive pulmonary disease: advances in the past 100 years. Am J Respir Cell Mol Biol 2005, 32:367–372
5. Finkelstein R, Fraser RS, Ghezzo H, Cosio MG: Alveolar inflammation and its relation to emphysema in smokers. Am J Respir Crit Care Med 1995, 152:1666–1672
6. Shapiro SD: The macrophage in chronic obstructive pulmonary disease. Am J Respir Crit Care Med 1999, 160:S29–S32
7. Di Stefano A, Capelli A, Lusuardi M, Balbo P, Vecchio C, Maestrelli P, Mapp CE, Fabbri LM, Donner CF, Saetta M: Severity of airflow limitation is associated with severity of airway inflammation in smokers. Am J Respir Crit Care Med 1998, 158:1277–1285
8. O'Shaughnessy TC, Ansari TW, Barnes NC, Jeffery PK: Inflammation in bronchial biopsies of subjects with chronic bronchitis: inverse relationship of CD8+ T lymphocytes with FEV1. Am J Respir Crit Care Med 1997, 155:852–857
9. Saetta M, Di Stefano A, Turato G, Facchini FM, Corbino L, Mapp CE, Maestrelli P, Ciaccia A, Fabbri LM: CD8+ T-lymphocytes in peripheral airways of smokers with chronic obstructive pulmonary disease. Am J Respir Crit Care Med 1998, 157:822–826
10. Saetta M, Baraldo S, Corbino L, Turato G, Braccioni F, Rea F, Cavallesco G, Tropeano G, Mapp CE, Maestrelli P, Ciaccia A, Fabbri LM: CD8+ve cells in the lungs of smokers with chronic obstructive pulmonary disease. Am J Respir Crit Care Med 1999, 160:711–717
11. Shapiro SD, Goldstein NM, Houghton AM, Kobayashi DK, Kelley D, Belaaouaj A: Neutrophil elastase contributes to cigarette smoke-induced emphysema in mice. Am J Pathol 2003, 163:2329–2335
12. Shapiro SD, Senior RM: Matrix metalloproteinases. Matrix degradation and more. Am J Respir Cell Mol Biol 1999, 20:1100–1102
13. Demedts IK, Bracke KR, Van Pottelberge G, Testelmans D, Verleden GM, Vermassen FE, Joos GF, Brusselle GG: Accumulation of dendritic cells and increased CCL20 levels in the airways of patients with chronic obstructive pulmonary disease. Am J Respir Crit Care Med 2007, 175:998–1005
14. Bracke KR, D'Hulst AI, Maes T, Moerloose KB, Demedts IK, Lebecque S, Joos GF, Brusselle GG: Cigarette smoke-induced pulmonary inflammation and emphysema are attenuated in CCR6-deficient mice. J Immunol 2006, 177:4350–4359
15. Saetta M, Mariani M, Panina-Bordignon P, Turato G, Buonsanti C, Baraldo S, Bellettato CM, Papi A, Corbetta L, Zuin R, Sinigaglia F, Fabbri LM: Increased expression of the chemokine receptor CXCR3 and its ligand CXCL10 in peripheral airways of smokers with chronic obstructive pulmonary disease. Am J Respir Crit Care Med 2002, 165:1404–1409
16. Grumelli S, Corry DB, Song LZ, Song L, Green L, Huh J, Hacken J, Espada R, Bag R, Lewis DE, Kheradmand F: An immune basis for lung parenchymal destruction in chronic obstructive pulmonary disease and emphysema. PLoS Med 2004, 1:e8
17. Ning W, Li CJ, Kaminski N, Feghali-Bostwick CA, Alber SM, Di YP, Otterbein SL, Song R, Hayashi S, Zhou Z, Pinsky DJ, Watkins SC, Pilewski JM, Sciurba FC, Peters DG, Hogg JC, Choi AM: Comprehensive gene expression profiles reveal pathways related to the pathogenesis of chronic obstructive pulmonary disease. Proc Natl Acad Sci USA 2004, 101:14895–14900
18. Bazan JF, Bacon KB, Hardiman G, Wang W, Soo K, Rossi D, Greaves DR, Zlotnik A, Schall TJ: A new class of membrane-bound chemokine with a CX3C motif. Nature 1997, 385:640–644
19. Imai T, Hieshima K, Haskell C, Baba M, Nagira M, Nishimura M, Kakizaki M, Takagi S, Nomiyama H, Schall TJ, Yoshie O: Identification and molecular characterization of fractalkine receptor CX3CR1, which mediates both leukocyte migration and adhesion. Cell 1997, 91:521–530
20. Ancuta P, Rao R, Moses A, Mehle A, Shaw SK, Luscinskas FW, Gabuzda D: Fractalkine preferentially mediates arrest and migration of CD16+ monocytes. J Exp Med 2003, 197:1701–1707
21. Lucas AD, Chadwick N, Warren BF, Jewell DP, Gordon S, Powrie F, Greaves DR: The transmembrane form of the CX3CL1 chemokine fractalkine is expressed predominantly by epithelial cells in vivo. Am J Pathol 2001, 158:855–866
22. Papadopoulos EJ, Sassetti C, Saeki H, Yamada N, Kawamura T, Fitzhugh DJ, Saraf MA, Schall T, Blauvelt A, Rosen SD, Hwang ST: Fractalkine, a CX3C chemokine, is expressed by dendritic cells and is up-regulated upon dendritic cell maturation. Eur J Immunol 1999, 29:2551–2559
23. Harrison JK, Jiang Y, Chen S, Xia Y, Maciejewski D, McNamara RK, Streit WJ, Salafranca MN, Adhikari S, Thompson DA, Botti P, Bacon KB, Feng L: Role for neuronally derived fractalkine in mediating interactions between neurons and CX3CR1-expressing microglia. Proc Natl Acad Sci USA 1998, 95:10896–10901
24. Yoshikawa M, Nakajima T, Matsumoto K, Okada N, Tsukidate T, Iida M, Otori N, Haruna S, Moriyama H, Imai T, Saito H: TNF-alpha and IL-4 regulate expression of fractalkine (CX3CL1) as a membrane-anchored proadhesive protein and soluble chemotactic peptide on human fibroblasts. FEBS Lett 2004, 561:105–110
25. Kanazawa N, Nakamura T, Tashiro K, Muramatsu M, Morita K, Yoneda K, Inaba K, Imamura S, Honjo T: Fractalkine and macrophage-derived chemokine: T cell-attracting chemokines expressed in T cell area dendritic cells. Eur J Immunol 1999, 29:1925–1932
26. Niess JH, Brand S, Gu X, Landsman L, Jung S, McCormick BA, Vyas JM, Boes M, Ploegh HL, Fox JG, Littman DR, Reinecker HC: CX3CR1-mediated dendritic cell access to the intestinal lumen and bacterial clearance. Science 2005, 307:254–258
27. Combadiere C, Salzwedel K, Smith ED, Tiffany HL, Berger EA, Murphy PM: Identification of CX3CR1. A chemotactic receptor for the human CX3C chemokine fractalkine and a fusion coreceptor for HIV-1. J Biol Chem 1998, 273:23799–23804
28. Combadiere C, Gao J, Tiffany HL, Murphy PM: Gene cloning, RNA distribution, and functional expression of mCX3CR1, a mouse chemotactic receptor for the CX3C chemokine fractalkine. Biochem Biophys Res Commun 1998, 253:728–732
29. Teupser D, Pavlides S, Tan M, Gutierrez-Ramos JC, Kolbeck R, Breslow JL: Major reduction of atherosclerosis in fractalkine (CX3CL1)-deficient mice is at the brachiocephalic artery, not the aortic root. Proc Natl Acad Sci USA 2004, 101:17795–17800
30. Lesnik P, Haskell CA, Charo IF: Decreased atherosclerosis in CX3CR1−/− mice reveals a role for fractalkine in atherogenesis. J Clin Invest 2003, 111:333–340
31. Bjerkeli V, Damas JK, Fevang B, Holter JC, Aukrust P, Froland SS: Increased expression of fractalkine (CX3CL1) and its receptor. CX3CR1, in Wegener's granulomatosis possible role in vascular inflammation. Rheumatology (Oxford) 2007, 46:1422–1427
32. Yano R, Yamamura M, Sunahori K, Takasugi K, Yamana J, Kawashima M, Makino H: Recruitment of CD16+ monocytes into synovial tissues is mediated by fractalkine and CX3CR1 in rheumatoid arthritis patients. Acta Med Okayama 2007, 61:89–98
33. Slebos DJ, Ryter SW, van der Toorn M, Liu F, Guo F, Baty CJ,

Karlsson JM, Watkins SC, Kim HP, Wang X, Lee JS, Postma DS, Kauffman HF, Choi AM: Mitochondrial localization and function of heme oxygenase-1 in cigarette smoke-induced cell death. Am J Respir Cell Mol Biol 2007, 36:409–417
34. Rangasamy T, Cho CY, Thimmulappa RK, Zhen L, Srisuma SS, Kensler TW, Yamamoto M, Petrache I, Tuder RM, Biswal S: Genetic ablation of Nrf2 enhances susceptibility to cigarette smoke-induced emphysema in mice. J Clin Invest 2004, 114:1248–1259
35. Witschi H, Espiritu I, Maronpot RR, Pinkerton KE, Jones AD: The carcinogenic potential of the gas phase of environmental tobacco smoke. Carcinogenesis 1997, 18:2035–2042
36. Witschi H, Espiritu I, Peake JL, Wu K, Maronpot RR, Pinkerton KE: The carcinogenicity of environmental tobacco smoke. Carcinogenesis 1997, 18:575–586
37. Jung S, Aliberti J, Graemmel P, Sunshine MJ, Kreutzberg GW, Sher A, Littman DR: Analysis of fractalkine receptor CX(3)CR1 function by targeted deletion and green fluorescent protein reporter gene insertion. Mol Cell Biol 2000, 20:4106–4114
38. Lee JS, Wurfel MM, Matute-Bello G, Frevert CW, Rosengart MR, Ranganathan M, Wong VW, Holden T, Sutlief S, Richmond A, Peiper S, Martin TR: The Duffy antigen modifies systemic and local tissue chemokine responses following lipopolysaccharide stimulation. J Immunol 2006, 177:8086–8094
39. Dunnill M: Quantitative methods in the study of pulmonary pathology. Thorax 1962, 17:320–328
40. Lee JS, Frevert CW, Matute-Bello G, Wurfel MM, Wong VA, Lin SM, Ruzinski J, Mongovin S, Goodman RB, Martin TR: TLR-4 pathway mediates the inflammatory response but not bacterial elimination in E. coli pneumonia. Am J Physiol 2005, 289:L731–L738
41. George CL, Jin H, Wohlford-Lenane CL, O'Neill ME, Phipps JC, O'Shaughnessy P, Kline JN, Thorne PS, Schwartz DA: Endotoxin responsiveness and subchronic grain dust-induced airway disease. Am J Physiol 2001, 280:L203–L213
42. Guerassimov A, Hoshino Y, Takubo Y, Turcotte A, Yamamoto M, Ghezzo H, Triantafillopoulos A, Whittaker K, Hoidal JR, Cosio MG: The development of emphysema in cigarette smoke-exposed mice is strain dependent. Am J Respir Crit Care Med 2004, 170:974–980
43. Teramoto S, Fukuchi Y, Uejima Y, Teramoto K, Oka T, Orimo H: A novel model of senile lung: senescence-accelerated mouse (SAM). Am J Respir Crit Care Med 1994, 150:238–244
44. Teramoto S, Uejima Y, Oka T, Teramoto K, Matsuse T, Ouchi Y, Fukuchi Y: Effects of chronic cigarette smoke inhalation on the development of senile lung in senescence-accelerated mouse. Res Exp Med (Berl) 1997, 197:1–11
45. Landsman L, Varol C, Jung S: Distinct differentiation potential of blood monocyte subsets in the lung. J Immunol 2007, 178:2000–2007
46. Fogg DK, Sibon C, Miled C, Jung S, Aucouturier P, Littman DR, Cumano A, Geissmann F: A clonogenic bone marrow progenitor specific for macrophages and dendritic cells. Science 2006, 311:83–87
47. Niewoehner DE, Kleinerman J, Rice DB: Pathologic changes in the peripheral airways of young cigarette smokers. N Engl J Med 1974, 291:755–758
48. Wallace WA, Gillooly M, Lamb D: Intra-alveolar macrophage numbers in current smokers and non-smokers: a morphometric study of tissue sections. Thorax 1992, 47:437–440
49. Welgus HG, Campbell EJ, Cury JD, Eisen AZ, Senior RM, Wilhelm SM, Goldberg GI: Neutral metalloproteinases produced by human mononuclear phagocytes. Enzyme profile, regulation, and expression during cellular development. J Clin Invest 1990, 86:1496–1502
50. Meucci O, Fatatis A, Simen AA, Miller RJ: Expression of CX3CR1 chemokine receptors on neurons and their role in neuronal survival. Proc Natl Acad Sci USA 2000, 97:8075–8080
51. Cardona AE, Pioro EP, Sasse ME, Kostenko V, Cardona SM, Dijkstra IM, Huang D, Kidd G, Dombrowski S, Dutta R, Lee JC, Cook DN, Jung S, Lira SA, Littman DR, Ransohoff RM: Control of microglial neurotoxicity by the fractalkine receptor. Nat Neurosci 2006, 9:917–924
52. Boehme SA, Lio FM, Maciejewski-Lenoir D, Bacon KB, Conlon PJ: The chemokine fractalkine inhibits Fas-mediated cell death of brain microglia. J Immunol 2000, 165:397–403
53. Geissmann F, Jung S, Littman DR: Blood monocytes consist of two principal subsets with distinct migratory properties. Immunity 2003, 19:71–82
54. Srivastava M, Meinders A, Steinwede K, Maus R, Lucke N, Buhling F, Ehlers S, Welte T, Maus UA: Mediator responses of alveolar macrophages and kinetics of mononuclear phagocyte subset recruitment during acute primary and secondary mycobacterial infections in the lungs of mice. Cell Microbiol 2007, 9:738–752
55. Havenith CE, Breedijk AJ, van Miert PP, Blijleven N, Calame W, Beelen RH, Hoefsmit EC: Separation of alveolar macrophages and dendritic cells via autofluorescence: phenotypical and functional characterization. J Leukoc Biol 1993, 53:504–510
56. Grayson MH, Ramos MS, Rohlfing MM, Kitchens R, Wang HD, Gould A, Agapov E, Holtzman MJ: Controls for lung dendritic cell maturation and migration during respiratory viral infection. J Immunol 2007, 179:1438–1448
57. Hautamaki RD, Kobayashi DK, Senior RM, Shapiro SD: Requirement for macrophage elastase for cigarette smoke-induced emphysema in mice. Science 1997, 277:2002–2004
58. Fraticelli P, Sironi M, Bianchi G, D'Ambrosio D, Albanesi C, Stoppacciaro A, Chieppa M, Allavena P, Ruco L, Girolomoni G, Sinigaglia F, Vecchi A, Mantovani A: Fractalkine (CX3CL1) as an amplification circuit of polarized Th1 responses. J Clin Invest 2001, 107:1173–1181
59. Sethi S, Murphy TF: Bacterial infection in chronic obstructive pulmonary disease in 2000: a state-of-the-art review. Clin Microbiol Rev 2001, 14:336–363